BUDOWNICTWO
CZASOPISMO TECHNICZNE
TECHNICAL TRANSACTIONS
CIVIL ENGINEERING
WYDAWNICTWO POLITECHNIKI KRAKOWSKIEJ
2-B/2012
ZESZYT 3
ROK 109
ISSUE 3
YEAR 109

BORIS BIELEK, MILAN BIELEK, JÁN SZABÓ, STANISLAV MIKLE*

THE VERIFICATION OF THE FUNCTION OF A NARROW-CAVITY DOUBLE-SKIN TRANSPARENT FAÇADE – *IN SITU* EXPERIMENT

WERYFIKACJA FUNKCJI WĄSKOSZCZELINOWEJ PRZEJRZYSTEJ FASADY PODWÓJNEJ – EKSPERYMENT *IN SITU*

Abstract

A tall slab-shaped building in north-south orientation. A narrow-cavity double-skin transparent façade. The south (S) external wall with the application of a double-skin transparent façade. The north (N) external wall with the application of a conventional transparent façade. The energy mode of a narrow-cavity double-skin transparent facade in summer. The function of a double-skin transparent facade and its impact on the energy mode of the indoor climate of adjacent spaces. In situ experiment and its documentation.

Keywords: double-skin transparent façade, narrow cavity, in situ experiment

Streszczenie

Wysoki budynek w kształcie płyty o północno-południowym kierunku ustawienia. Wąskoszczelinowa przejrzysta fasada podwójna. Południowa ściana zewnętrzna z przejrzystą fasadą podwójną. Północna ściana zewnętrzna z przejrzystą fasadą konwencjonalną. Tryb energetyczny wąskoszczelinowej przejrzystej fasady podwójnej w okresie letnim. Funkcja przejrzystej fasady podwójnej i jej wpływ na tryb energetyczny wewnętrznego klimatu przyległych przestrzeni. Eksperyment *in situ* wraz z dokumentacją.

Słowa kluczowe: przejrzysta fasada podwójna, wąska szczelina, eksperyment in situ

* PhD. Doc. Eng. Boris Bielek, Prof. DSc. Eng. Milan Bielek, Eng. Ján Szabó, Eng. Stanislav Mikle, Faculty of Civil Engineering, Slovak University of Technology.

1. Introduction to the problem

For the renovation of the façade of a tall slab-shaped building (23 floors above the ground), it was decided to apply a double-skin transparent façade on the south side and a conventional light transparent façade on the north side. There is a corridor area between office spaces adjoining the southern and northern facades to which these office spaces are connected only by the doors (they are not connected directly, by cross ventilation for instance). The subject of interest in this paper will be just the south wing of the building adjacent to the southern double-skin façade consisting of panels made of glass and aluminium alloys with systems consistently breaking thermal bridges constructed in the system SAPA Thermo 74 SX (Fig.1). The transparent parts of the internal skin of the double-skin façade consist of win-

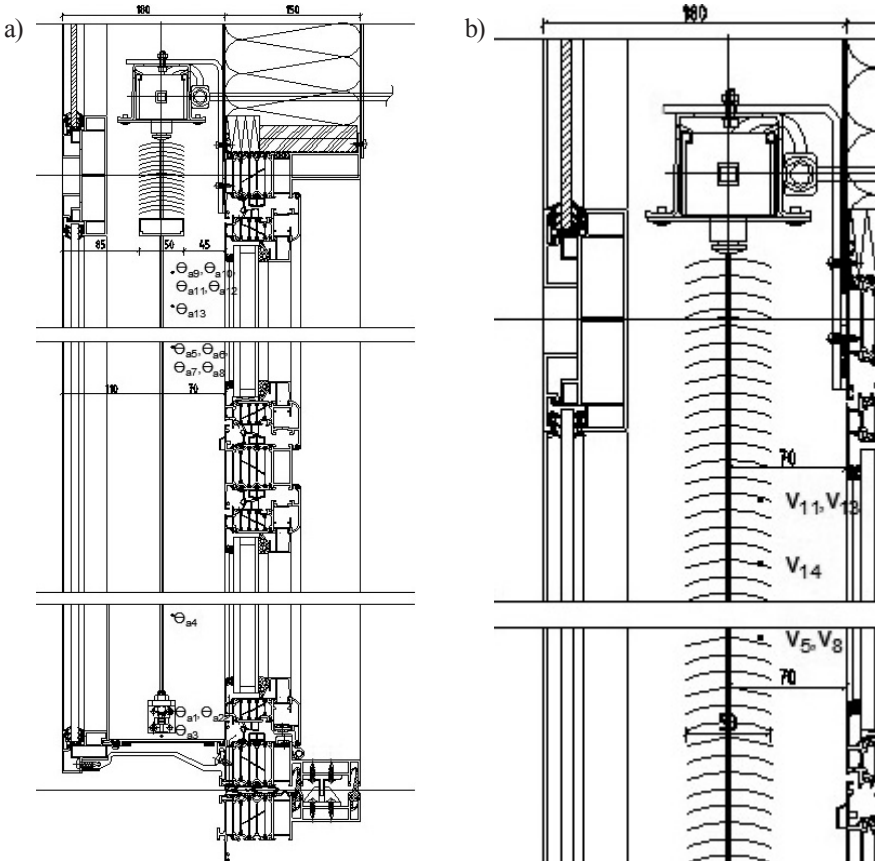

Fig. 1. Vertical section through double-skin transparent façade: a) position of measuring points for air temperature in the cavity $\theta_{a,x}$ (ºC) in relation to the structure of the cavity, b) position of measuring points for air flow velocity v_x (m/s) in relation to the structure of the cavity

Rys. 1. Przekrój pionowy przejrzystej fasady podwójnej: a) pozycja punktów pomiarowych temperatury powietrza w szczelinie $\theta_{a,x}$ (ºC) w stosunku do struktury szczeliny, b) pozycja punktów pomiarowych prędkości przepływu powietrza v_x (m/s) w stosunku do struktury szczeliny

dows with frame profiles of thermal quantification U_f = 2.4-2.8 W/m²·K and insulated double glazed units (6-16-4) of thermal quantification U_g = 1.1 W/m²·K. The opaque parts of the internal skin of the double-skin façade consist of sills with highly efficient thermal insulation material (mineral wool, 150 mm thick) covered by cladding panels (gypsum, Al-sheets) and highly effective diffusion retarders and air barriers in the form of foil with the overall thermal quantification U_{sill} = 0.25 W/m²·K. The overall area average heat transfer coefficient of the internal skin of the double-skin façade has the value of U_m = 1.17 W/m².K. The geometrical parameters of the assembled panel of the double-skin façade and the geometrical parameters of the cross section of air flow trajectory in the physical cavity are shown in Fig. 2.

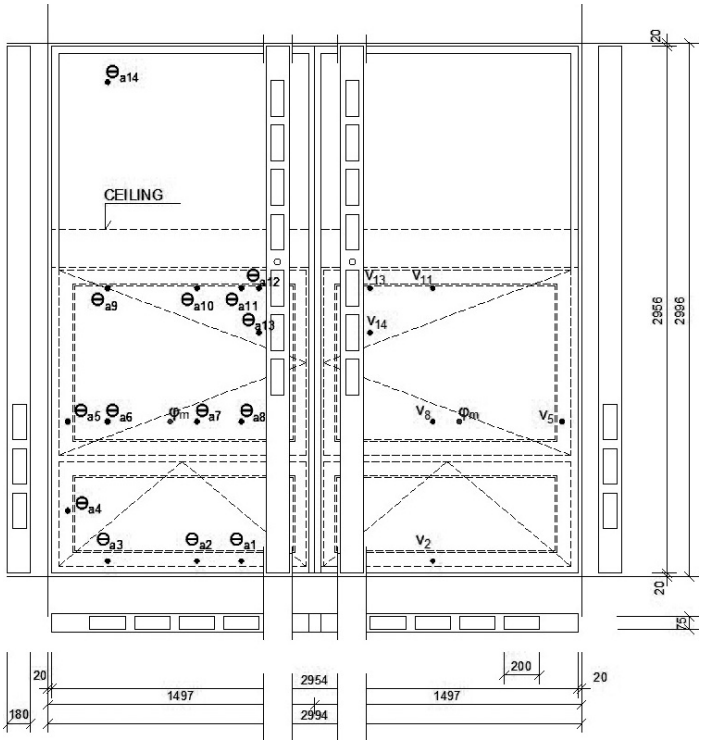

Fig. 2. Vertical scheme of physical cavity (width b = 180 mm) of assembled panel of double-skin façade showing location of air inlet and air outlet openings. Scheme of location of measuring points for monitored parameters of natural physical cavity in assembled panel of double-skin facade: θa,x – measuring points for temperature monitoring (ºC), vx – measuring points for wind speed monitoring (m/s), φ_m – measuring points for relative air humidity monitoring (%)

Rys. 2. Pionowy schemat szczeliny fizycznej (szerokość b = 180 mm) złożonego panelu przejrzystej fasady podwójnej ukazujący lokalizację otworów wlotu i wylotu powietrza. Schemat lokalizacji punktów pomiarowych dla monitorowanych parametrów naturalnej szczeliny fizycznej w złożonym panelu fasady podwójnej: $\theta_{a,x}$ – punkty pomiarowe dla monitoringu temperatury (ºC), v_x – punkty pomiarowe dla monitoringu prędkości wiatru (m/s), φ_m – punkty pomiarowe dla monitoringu względnej wilgotności powietrza (%)

2. The subject, objectives and methodology of the problem

The subject of the problem is a double-skin transparent façade consisting of assembled façade panels with a narrow cavity [1] whose width b = 180 mm (Fig. 2) that is applied to a tall slab-shaped building in the area of Bratislava.

The objective of the problem, associated with the verification of the functionality of this transparent double-skin façade, is the physical quantification of the energy mode of its narrow cavity in basic operating modes that are associated with the operation of windows on the internal wall of the façade and with the operation of the sun protection system in the cavity of the façade (Fig. 1), in both cases under the influence of the subjective factor of a user. This fundamental objective will facilitate the recommendation of the optimal operation mode for the façade in the summer.

The methodology for the problem is based on an in situ experiment in order to obtain the parameters of the energy mode in the cavity of the façade. The in situ experiment was carried out in one measuring room (605) and two reference rooms (606 and607) – Fig. 3. The parameters of the energy mode of the cavity and the parameters of the indoor climate were monitored in the measuring room. In the reference rooms, only the parameters of the indoor climate were monitored. The outdoor climate parameters were monitored by a mobile meteorological station situated at the level of the measured façade with an adequate orientation (SW).

In terms of the operation of rooms, six series of measurement were performed in three modes (R):

Mode R1: windows on the internal skin are closed. This mode represents an extreme because the cavity is completely disconnected from the interior of the building – office spaces,

Mode R2: windows on the internal skin are open. This mode represents an extreme because the cavity is completely connected with the interior of the building,

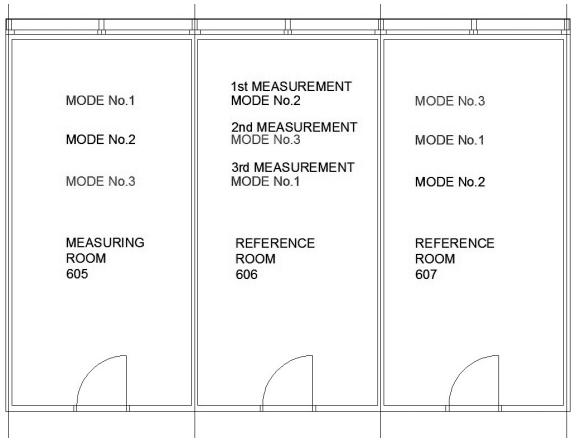

Fig. 3. Scheme of measuring methodology of 3 basic operation modes of the facade consisting of one measuring room and two reference rooms

Rys. 3. Schemat metodologii pomiarów 3 podstawowych trybów operacyjnych fasady złożony z jednego pomieszczenia pomiarowego i dwóch pomieszczeń ewidencyjnych

Mode R3: windows on the internal skin are open during dark hours of the day (from 08.00 p.m. to 08.00 a.m.) and closed during sunlight hours (from 08.00 a.m. to 08.00 p.m.). This mode represents minimal thermal load on the building from sunlight (day) and the recovery of heat storage in the building (night).

The series of measurements 1, 2 and3 were carried out in the cavity while the blinds were pulled down (sun protection in operation) – Fig. 1b. The series of measurements 4, 5 and6 were carried out in the cavity while blinds were pulled up (sun protection out of operation) – Fig. 1a.

3. The results of the in situ experiment

In accordance with the methodology of the in situ experiment and with the scheme shown in Fig. 3, 6, a basic series of measurement for the three modes were performed (R1, R2, R3).

A summary of the crucial physical parameters of the cavity, the outdoor climate and the indoor climate from the series of six basic in situ experiments, carried out in the summer of 2011, is shown in Table 1.

Table 1

Summary of physical parameters of outdoor climate (min θ_{ae} (°C), max θ_{ae} (°C), max I_m (W/m²), average $v_{w,300}$ (m/s)), physical cavity (max θ_{am} (°C), max $\Delta\theta_{am}$ (K)) and indoor climate (θ_{ai} (°C)) from a series of 6 in situ experiments in the summer of 2011

meas. series	R – ENERGY MODE OF FACADE																	
	R1						R1						R1					
Para-meter	min θ_{ae} (°C)	max θ_{ae} (°C)	max θ_{am} (°C)	max $\Delta\theta_{am}$ (K)	max I_m (W/m²)	avg $v_{w,300}$ (m/s)	min θ_{ae} (°C)	max θ_{ae} (°C)	max θ_{am} (°C)	max $\Delta\theta_{am}$ (K)	max I_m (W/m²)	avg $v_{w,300}$ (m/s)	min θ_{ae} (°C)	max θ_{ae} (°C)	max θ_{am} (°C)	max $\Delta\theta_{am}$ (K)	max I_m (W/m²)	avg $v_{w,300}$ (m/s)
1	+17	+30	+53	23	600	1,8	(606) $+23 \leq \theta_{ai}$(°C) $\leq +28$						(607) $+23 \leq \theta_{ai}$(°C) $\leq +25$ COMFORT					
	(605) $+25 \leq \theta_{ai}$(°C) $\leq +27$																	
2	(607) $+24 \leq \theta_{ai}$(°C) $\leq +26$						+12,5	+27	+49	22	650	1,7	(606) $+21{,}5 \leq \theta_{ai}$(°C) $\leq +25$ COMFORT					
							(605) $+22 \leq \theta_{ai}$(°C) $\leq +27$											
3	(606) $+26{,}5 \leq \theta_{ai}$(°C) $\leq +28$						(607) $+23{,}5 \leq \theta_{ai}$(°C) $\leq +31{,}5$						+16,5	+31,5	+53	21,5	650	3,3
													(605) $+24{,}5 \leq \theta_{ai}$(°C) $\leq +27{,}5$ LIMIT					
4	+22,5	+37	+55	18	650	2,3	(606) $+28{,}5 \leq \theta_{ai}$(°C) $\leq +37$						(607) $+28 \leq \theta_{ai}$(°C) $\leq +31{,}5$ DISCOMFORT					
	(605) $+29{,}5 \leq \theta_{ai}$(°C) $\leq +35{,}5$																	
5	(607) $+29 \leq \theta_{ai}$(°C) $\leq +33$						+14,5	+31,5	+50	18,5	700	1,2	(606) $+26{,}5 \leq \theta_{ai}$(°C) $\leq +32{,}5$ DISCOMFORT					
							(605) $+26{,}5 \leq \theta_{ai}$(°C) $\leq +35$											
6	(606) $+27 \leq \theta_{ai}$(°C) $\leq +32$						(607) $+24{,}5 \leq \theta_{ai}$(°C) $\leq +34{,}5$						+15	+31	+53	22	700	1,7
													(605) $+25 \leq \theta_{ai}$(°C) $\leq +31{,}5$ DISCOMFORT					

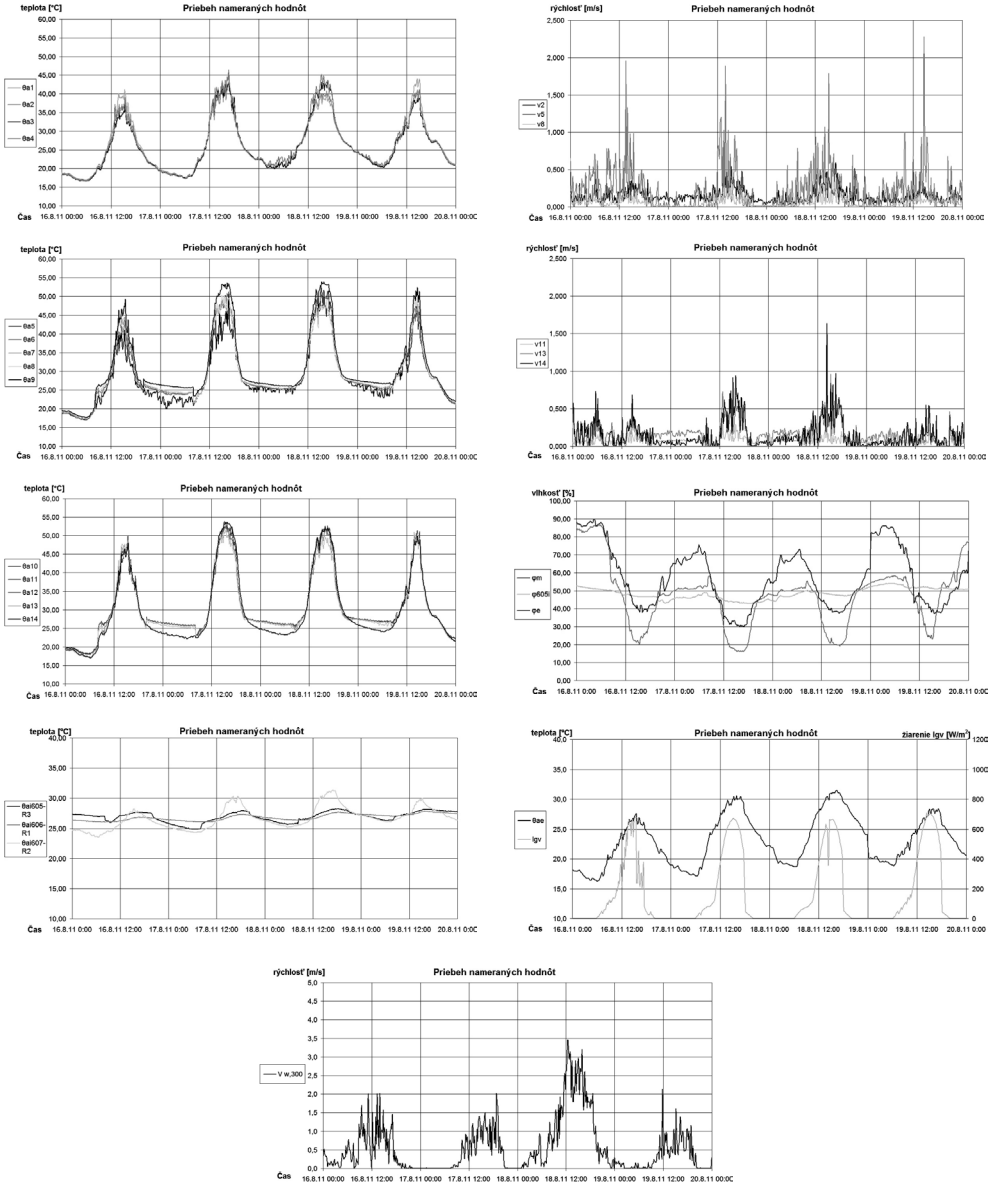

Fig. 4. Physical parameters monitored during in situ experiment used for quantification of energy mode of double-skin façade; Measurement series 3. Measuring room: mode R3 (window on internal skin is closed – open). Sun protection in operation (blinds pulled down)

Rys. 4. Parametry fizyczne monitorowane w trakcie eksperymentu in situ wykorzystywane do kwantyfikacji trybu energetycznego fasady podwójnej; Seria pomiaru 3. Pomieszczenie pomiarowe: tryb R3 (okno w warstwie wewnętrznej zamknięte – otwarte). Ochrona przeciwsłoneczna aktywna (żaluzje zaciągnięte)

4. The processing of the results of the in situ experiment

The natural physical cavity of the assembled panel of the double-skin transparent façade is due to:

- the relative complexity of air inlet and outlet openings – Fig. 2
- relatively small cross-sectional area of these openings ($\sum A_{OPENING} \approx 0.05$ m^2/ per metre of panel, compared to the NBS where $\sum A_{OPENING} \approx 0.16$ m^2/per metre of panel) and
- geometric disproportion of air exhaust from the cavity (from 2 panels and14 openings of area $\sum A_{OPENING} \approx 0.1$ m^2 into the collecting channel of cross-sectional area $A_{VERT\ CANAL} = 0.04 \,.\, 0.16 \approx 0.0064$ m^2)

characterized by high coefficients of the local aerodynamic resistance of air outlet and a high value of the total aerodynamic resistance of the physical cavity. The high value of the total aerodynamic resistance of the physical cavity is a prerequisite condition for the unwanted stagnation of air in the cavity under still air (Fig. 4). In this situation, the total aerodynamic resistance of the cavity has a higher value than convective air buoyancy in the cavity. The intervals of air stagnation in the cavity rank among the causes of high temperatures θ_{ai} (ºC) in the interior of the building.

If the average speed of airflow in the cavity is represented by $v_8 \approx 0.2$ m/s (Fig. 4), monitored approximately in the middle of the transparent part of the window of the assembled panel, volumetric airflow $q_V \approx 0.2\ (0.16 \,.\, 1.0) = 0.032$ m^3/s·m and mass airflow $q_m = q_V \cdot \rho_{(\theta)} \approx 0.032 \,.\, 1.317 \approx 0.04$ kg/s·m $<<$ 0.2 kg/s·m. This parameter informs us about the very low energy efficiency of the double-skin facade. This is another cause of high temperatures θ_{ai} (ºC) in the interior of the building.

The energy mode of the physical cavity is characterized by thermal mode θ_{ax} (ºC) best expressed by the profile of temperature rise in the cavity $\Delta\theta_{am}$ (K) in relation to the input temperature of the outdoor climate θ_{ae} (ºC). The profile of temperature rise in the natural physical cavity for all series of measurement is shown in Fig. 5.

5. Conclusions

A. The results of the in situ experiment in all series of measurement document the fact that the “most suitable” mode of façade operation for the typical summer max. $\theta_{ae} \geq 25$°C is mode R3 (windows closed – open) – Table 1, Fig. 6. In spite of that, it is necessary to point out that this façade mode R3 is not very efficient and is definitely not the optimal one. It would be the optimal mode if cross ventilation from the northern wing with a typical transparent façade was ensured during the dark hours of the day. The second ”less suitable“ mode is R1 (windows closed). Mode R2 is unsuitable (windows open) – Table 1, Fig. 6. Sun protection in the hours of direct sunlight is an efficient instrument for indoor climate creation for each of the analyzed façade modes, especially for mode R1 and mode R3.

B. In mode R3 and for temperatures of outdoor climate in the interval $25 \leq \theta_{ae}$ (°C) ≤ 30 and for the intensity of solar radiation $I_m \leq 650$ W/m^2, the analyzed façade provides thermal comfort in indoor climate (COMFORT) – Fig. 6, series of measurement 1 and2. For $\theta_{ae} > 30$°C and $I_m > 650$ W/m^2, it causes thermal discomfort in indoor cli-

mate (DISCOMFORT) – Fig. 6, series of measurement 3, the same applies even more so for series of measurement 4, 5 and 6 which are more critical – Table 1, Fig. 6. It is due to the fact that the sun protection is out of operation for these series of measurement – the blinds are pulled up.

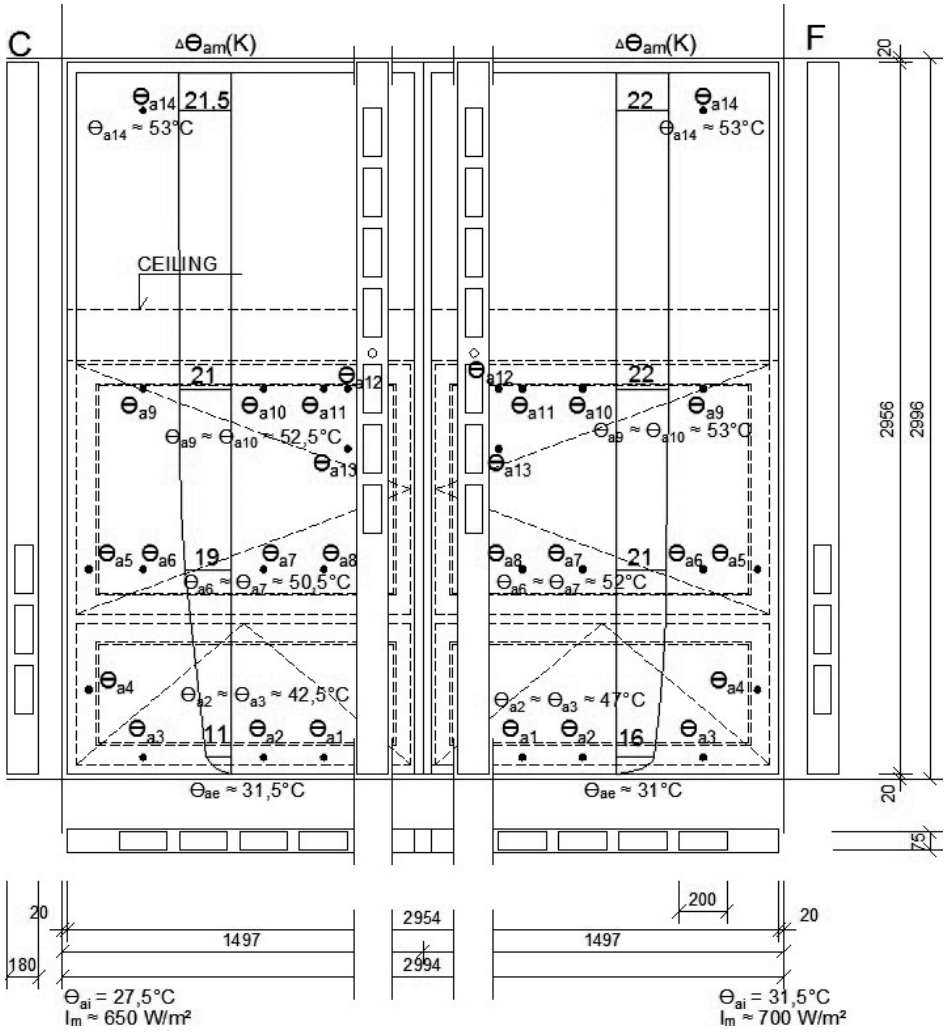

Fig. 5. Diagrams of air temperature increase in natural physical cavity of double-skin façade $\Delta\theta_{am}$ (K); C – Measurement series 3. Mode R3 (window on internal skin is closed – open). Sun protection in operation (blinds pulled down), F – Measurement series 6. Mode R3 (window on internal skin is closed – open). Sun protection out of operation (blinds pulled up)

Rys. 5. Diagramy wzrostu temperatury powietrza w naturalnej szczelinie fizycznej fasady podwójnej $\Delta\theta_{am}$ (K); C – Seria pomiarów 3. Tryb R3 (okno w warstwie wewnętrznej zamknięte – otwarte) Ochrona przeciwsłoneczna aktywna (żaluzje zaciągnięte), F – Seria pomiarów 6. Tryb R3 (okno w warstwie wewnętrznej zamknięte – otwarte). Ochrona przeciwsłoneczna nieaktywna (żaluzje podciągnięte)

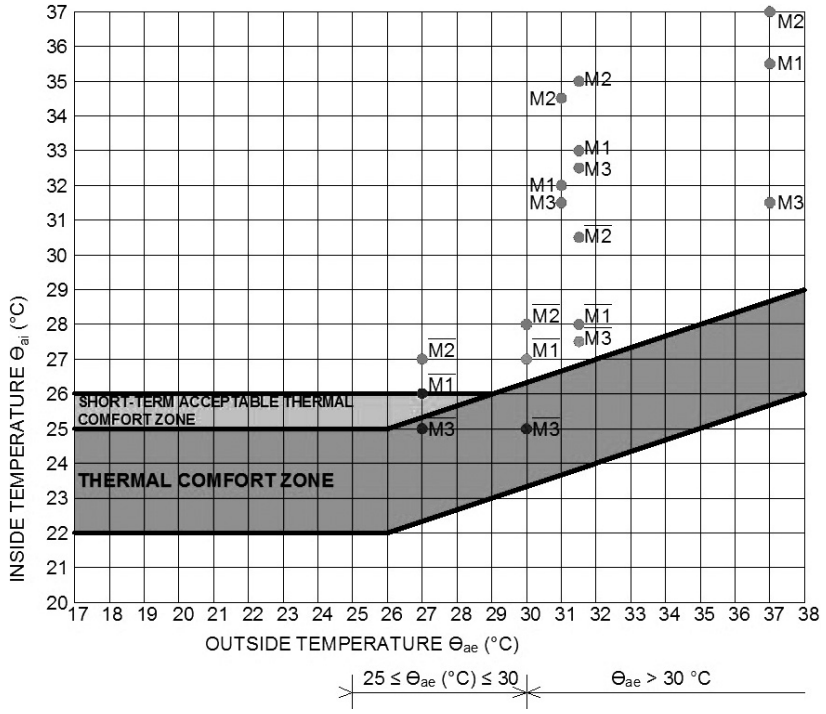

Fig. 6. Maximum temperatures of internal climate max θ_{ai} (°C) obtained by in situ experiment: in regime $\overline{R1}$, $\overline{R2}$, $\overline{R3}$ (blinds were pulled down – sun protection in operation) and in regime R1, R2, R3 (blinds were pulled up – sun protection out of operation). Interaction of air temperature of outdoor climate θ_{ae} (°C) and sensational temperature of comfort $\theta_{ai,c}$ (°C) for sedentary administrative work with light and average wear

Rys.6. Maksymalne temperatury klimatu wewnętrznego max θ_{ai} (°C) uzyskane w eksperymencie *in situ*: w trybie $\overline{R1}$, $\overline{R2}$, $\overline{R3}$ (żaluzje zaciągnięte – ochrona przeciwsłoneczna aktywna) i w trybie R1, R2, R3 (żaluzje podciągnięte – ochrona przeciwsłoneczna nieaktywna). Wzajemne oddziaływanie temperatury powietrza klimatu zewnętrznego θ_{ae} (°C) i odczuwalnej temperatury komfortu $\theta_{ai,c}$ (°C) dla siedzącej pracy administracyjnej wymagającej lekkiego i przeciętnego wysiłku

C. As a result of a geometric disproportion in the cross sections of airflow trajectory through the natural physical cavity of the double-skin façade, there is [1]:
   – high value of its total aerodynamic resistance causing the stagnation of air in the cavity under still air (the aerodynamic resistance of the cavity is higher than convective air buoyancy) [2],
   – low airflow rate through the cavity ($q_m \approx 0.04$ kg/s·m << 0.2 kg/s·m = $q_{m,\mathrm{REQUIRED}}$) [1, 3] causing the low-energy efficiency of the double-skin façade.

These two facts are responsible for high temperature rise in the physical cavity as well as the high air temperatures of indoor climate during the typical summer. They are caused by the underestimation of the physical dimensioning of the double-skin façade in two main interrelated and mutually influencing fields: in the field of aerodynamics [1] and in the field of solar thermal technology in buildings [3].

This work was supported by the Slovak Research and Development Agency under Contract No. APVV-0624-10.

Denotations

U	–	heat transmission coefficient (U-value), [W/(m^{2}K)]
A	–	area [m^2]
v	–	airflow velocity [m/s]
q_V	–	air flow rate in cavity [m^3/s]
q_m	–	mass flow rate in cavity [kg/s]
θ	–	temperature [°C]
$\Delta\theta_{am}$	–	high temperature rise in the cavity [K]
I_m	–	intensity of solar radiation [W/m^2]
ρ	–	apparent density [kg/m^3]

References

[1] Bielek B., Bielek M., Palko M., *Double skin transparent facades of buildings, 1st volume: History of development, classification and theory of structural design*, Coreal, Bratislava 2002.

[2] Bielek B., Bielek M., Kusý M., Paňák P., *Double skin transparent facades of buildings, 2nd volume: Development, simulation, experiment and construction design of the façade the NBS building in Bratislava*, Coreal, Bratislava 2002.

[3] Cihelka J., *Solar thermal technology*, Nakladatelství T. Malina, Prague 1994.

[4] Bielek M., Bielek B., *Climatic, ecological, energy and structural concept for facade modernization of Východočeská energetika building in Hradec Králové, In: Indoor climate of buildings 2009 – Environmental assessment of indoor environment of buildings*, Slovak Society for Environmental Technology, Bratislava 2009, 115-120.